

Power combination of two 140 GHz gyrotrons and fast switching of the combined beam

FS&T
Ms-343308
Recd: 5/16/08

V. Erckmann¹, W. Kasperek², Y. Koshurin³, L. Lubyako³, M.I. Petelin³,
D.Yu Shchegolkov³, F. Hollmann¹, G. Michel¹, F. Noke¹, F. Purps¹, ECRH
groups at IPP Greifswald¹, IPF Stuttgart², IAP Nizhny Novgorod³, FZK
Karlsruhe⁴, and IFP Milano⁵

¹Max-Planck-Institut für Plasmaphysik (IPP), EURATOM-Association, D-17491
Greifswald, Germany

²Institut für Plasmaforschung, Universität Stuttgart, Pfaffenwaldring 31, D-70569
Stuttgart, Germany

³Institute of Applied Physics, RAS, 603950 Nizhny Novgorod, Russia

⁴Forschungszentrum Karlsruhe, Association EURATOM-FZK, IHM, D-76021
Karlsruhe, Germany

⁵Istituto di Fisica del Plasma, EURATOM-ENEA-CNR Ass., via R. Cozzi 53,
20125 Milano, Italy

Information on the corresponding author:

Volker Erckmann
*Max Planck Institut für Plasmaphysik,
Wendelsteinstrasse 1, D-17491 Greifswald, Germany*
e-mail: volker.erckmann@ipp.mpg.de
cc to: walter.kasperek@ipf.uni-stuttgart.de

Phone: +49-3834-88-2450 Fax: +49-3834-88-2459

Pages: 14 (text only), 28 (including figures, captions and references)

Tables: 0

Figures: 9

Abstract

Experiments on the combination of the high power wave beams from two gyrotrons and fast switching of the combined beam between two transmission channels are described. The measurements were performed using a high-power resonator diplexer in the optical transmission line of the electron cyclotron heating system for W7-X. The principle and the engineering design of the prototype four-port quasi-optical diplexer is presented. The wave beams from two gyrotrons with an output power of 370 kW and 560 kW, respectively, have been combined for pulse lengths up to 10 seconds, only limited by the un-cooled mirrors used in the diplexer. By modulating the gyrotron frequency using a fast high-voltage body modulator, controlled toggling of the combined power between the two outputs of the diplexer was demonstrated with switching frequencies of up to 20 kHz.

The experiments are compared to theory, showing good agreement when the limited stability of the free-running gyrotrons is taken into account.

Key words: Diplexer, Power combiner, Millimeter Wave transmission, Electron cyclotron Heating.

PACS numbers: 52.50.Gj, 52.35.-g, 84.40.-x, 42.79.Ci

I. INTRODUCTION

Combining the power from two (or more) conventional gyrotrons would essentially reduce the number of transmission lines and launchers for electron cyclotron resonance heating (ECRH) and current drive (ECCD) systems of large fusion experiments [1]. This could be an interesting option for ITER, where an upgrade of the installed power is under discussion, while the number of available ports and thus the number of launchers remains limited. Power combiners can be composed of oversized four-port diplexers, the gyrotrons being implied to generate slightly different frequencies f_1 and f_2 .

High-power diplexers can be used also for fast switching of the power from a continuously operating gyrotron between two outputs. An application is the stabilization of neoclassical tearing modes [2], where toggling of the power between two launchers synchronous to the rotation (several kHz!) of the magnetic islands would increase the efficiency for stabilization significantly [3]. In general, fast switches allow sharing of the installed power between different types of launchers or different applications depending on priority. The switching is based on a small frequency-shift keying of the gyrotron between f_1 and f_2 performed by modulation of the gun anode or the beam acceleration voltage, making use of the steep transmission characteristics of the diplexer [4]. Note that for the tiny frequency shifts $f_1 - f_2 = \Delta f_s$ of some tens of MHz needed for the switching, no remarkable change of the deposition radius in the plasma occurs. When two gyrotrons are fed into a four-port diplexer, and both gyrotrons are shifted between frequencies f_1 and f_2 , then the power of both gyrotrons can be combined into one of the two outputs, and switched between output 1 and 2 in the rhythm of the frequency-shift keying.

If diplexers are used with free-running gyrotrons, a tuning element (movable mirror) might be needed to match the transmission characteristics to (slow variations of) the gyrotron frequency. Slow switching between two outputs is always possible by moving the tuning

mirror by typically a half wavelength. This could be interesting for applications, where frequency variation by HV-modulation is not possible, but where the gyrotron should not be switched off during the switching process (e.g. for "hot stand-by"), or a variable splitting ratio of the power is envisaged.

To demonstrate the possibilities and investigate the performance of high-power diplexers in ECRH systems, a prototype based on a compact quasi-optical cavity was set up. This diplexer had been characterized before with low power by various methods [5, 6]. After passing these tests, it was integrated in the quasi-optical transmission line of the 10 MW, cw ECRH system, which is under construction for the stellarator W7-X at IPP Greifswald [7]. First tests demonstrated the switching performance of this device [6], using frequency-shift keying of the 140 GHz gyrotron wave beam fed to its input. In this paper, we show experiments on power combination from two gyrotrons as well as first experiments on fast switching of the combined millimetre wave beam between the two outputs.

II. EXPERIMENTAL SET UP

IIa. Diplexer design and installation

The principle design for the resonant diplexer is sketched in figure 1. It consists of a quasi-optical ring resonator with a high Q-factor with two integrated diffraction gratings as input and output couplers. If we denote the grating efficiencies for 0th order as R_0 , for -1st order as R_1 , and the round-trip efficiency of the unloaded resonator as R_q , then the power transmission coefficients from the input 1 to output 1 and 2, respectively, are given by

$$T_1(f) = R_0 \cdot \frac{1 + R_q - 2\sqrt{R_q} \cdot \cos(2\pi Lf/c)}{1 + R_0^2 R_q - 2\sqrt{R_q} R_0 \cdot \cos(2\pi Lf/c)} \quad (1)$$

$$T_2(f) = \frac{R_1^2 \sqrt{R_q}}{1 + R_0^2 R_q - 2\sqrt{R_q} R_0 \cdot \cos(2\pi Lf/c)} \quad (2)$$

with $R_0 + R_1 = 1$, and the resonator length L , frequency f and the speed of light c . Note that all angles of incidence and diffraction on the grating are equal (45° in the present design).

For the experiments, a mock-up diplexer using un-cooled aluminium mirrors had been constructed [5, 6]. The (measured) parameters are as follows: Length of resonator $L = 2386$ mm, coupling gratings with period $p = 2.14$ mm, grating efficiencies in 0th and -1st order of $R_0 = 0.78$ and $R_1 = 0.22$, and $R_q \geq 0.986$, respectively. This results in a transmission in the non-resonant channel with periodic notches and in the resonant channel with periodic resonances, respectively, separated by $c/L = 125.6$ MHz ("free spectral range"). The corresponding transmission curves which were confirmed in low-power tests [6] are shown in Fig. 2. For power combination, one beam is injected at input 1 with the resonant frequency f_2 , the other beam is injected at input 2 with the non-resonant frequency f_1 (see also Fig. 1). Thus, both beams exit at output 2. Exchanging these frequencies would result in coupling of the total power to output 1.

One out of the four ring-resonator mirrors was equipped with 3 mike drives for remote control of the alignment as well as fine tuning of the resonance frequencies according to the gyrotron frequencies. Note that a movement of one resonator mirror normal to its surface by $\Delta z = \lambda/2 = 1.51$ mm would produce a shift of the resonance corresponding to a free spectral range, i.e. 125.6 MHz. The resulting misalignment of the resonator is still tolerable.

For the experiments, the ECRH transmission system for W7-X at IPP Greifswald [7] was used. The complete set up is shown in Fig. 3. This system features two symmetric multi-beam transmission lines with 5 MW each, allocated to the modules 1 and 5 of the stellarator. This system allows to simultaneously inject any one beam out of the (finally) five 140- GHz gyrotrons of each module into two CW calorimetric loads, designated as CCR1 and CCR5. For the experiments, the two prototype gyrotrons “B1” in module 1 and “B5” in module 5 manufactured by Thales Electron Devices [8] were fed to the diplexer. These gyrotrons have a potential depressed collector; their acceleration voltage and thus the output power are controlled by a fast HV modulator [9]. The diplexer was installed between the last focussing mirrors (MD1 and MD5), and the entrance to the loads. For the incident beams from the gyrotrons and the two output beams to the loads, 2 matching mirrors each were installed to adapt the diplexer resonator to the parameters of the beams between mirrors MD and the load entrances. The beam path for both beams is sketched in Fig. 3. Note that the grating efficiency of the coupling gratings in the diplexer given above and thus the transmission function (Fig. 2) is valid for the TE polarization (E-field parallel to the grooves). In the experiments, this was taken into account by adjusting the proper polarization with the polarizers in the transmission lines.

II.b Diagnostics

The alignment of the beams was performed by thermal imaging of the beam pattern on absorbing PVC plates installed at appropriate positions. For the experiments, a set of diagnostic tools was available:

Power monitors (designated IN1 and IN5 in the following) are installed on the first mirror (M1) of the ECRH-transmission line [7] after the output window of the gyrotrons. Directly behind M1, the beams can be coupled to a calorimetric load with a switching mirror for calibration of IN1 and IN5. A second set of power monitors (designated OUT1 and OUT5 in the following) is installed at the last matching mirror of the diplexer directly in front of the CW loads, which serve for calibration here. Note that the power monitor signals (predominantly in the first second of the pulses, and especially output coupler OUT1) suffered from interference by stray radiation, therefore, the average over the complete pulse was used for calibration.

The CW calorimetric loads feature a delay of response (due to the finite water flow rate) of about 5 s plus a thermal time constant of about 7 s, therefore the integral over the heat pulse and the information from the flow meters was taken for power measurement.

For recording of the frequency characteristics of the gyrotrons, a down-converter with a local oscillator frequency of $f_{LO} = 139.65$ GHz, followed by a Hewlett Packard 5372A frequency analyzer was installed. It was connected to simple horn couplers near to the gyrotron output window. Frequency measurements on the gyrotrons B1 and B5 show the following behaviour: For about 0.5 s after switch-on, the gyrotrons exhibit a frequency chirp of up to 360 MHz (figure 6a), which is due to heating and thermal expansion of the cavity. The total chirp is practically proportional to the output power of the tubes. After thermalization of the cavity (> 1 s), the frequency is very stable and drifts only when the power is varying. In addition, we observe spontaneous frequency jumps of the order of a few MHz, probably initiated by a

change of internal reflection conditions back to the cavity ("frequency-pulling", "long-line-effect"). Over pulse lengths of 10 s, the gyrotron B1 was stable within typically ± 4 MHz. Gyrotron B5 showed more frequency jumps yielding a stability of typically ± 8 MHz. The instantaneous line-width of the gyrotron is always much less than 1 MHz; the broadening of the frequency seen in the plots is due a modulation of the LO frequency (± 1.8 MHz) caused by 50-Hz noise on the power supply.

III. POWER COMBINATION EXPERIMENTS

The gyrotrons were operated with a power up to 600 kW each for the power combination experiments. It should be noted, that the combined power had to be kept below 1 MW, which is the power limit for the dummy load. . At this level, the diplexer operated without remarkable problems and only a few arcs were detected, although the maximum power density in the beam near to the grating surface was ≥ 0.5 MW/cm², which is to be compared with the theoretical arcing limit in normal atmosphere of 1 MW/cm². As un-cooled Al mirrors are used even in the resonator, we have limited the pulse length to 3 s; for some selected experiments the pulse lengths was extended up to 10 s.

The monotonic dependence of the total frequency chirp from the output power was used to adjust the difference frequency of the gyrotrons (for pulse time > 1 s) to a value of typically 40 MHz. The position of the motorized resonator mirrors was adjusted such that a resonance of the diplexer was identical to one of the gyrotron frequencies.

A basic experiment is shown in Figures 4 and 5. The diplexer resonance is set to a frequency of 140.245 GHz corresponding to the frequency of 595 MHz in the scale of the frequency analyzer, which is used in the following. At the end of the 3-s pulse, the frequency of gyrotron B1 is resonant, gyrotron B5 is non-resonant. When gyrotron B1 is pulsed (Fig. 4),

it starts the pulse at a non-resonant frequency (about 780 MHz), goes through the diplexer resonance at 721 MHz, and finally stabilizes at the resonance at 595 MHz. Thus the power leaves the diplexer mainly at output 5. From the signals OUT1 and OUT 5, one can clearly see the transition of the power from the non-resonant to the resonant channel for $0.8 \text{ s} < t < 2 \text{ s}$, including the effect of frequency jumps seen in the corresponding frequency measurement. Note the large ratio of the powers detected by OUT5 and OUT 1 during the major period of the pulse ($1 \text{ s} < t < 3 \text{ s}$) of 0.91 : 0.09, and even 0.98 : 0.02 during the last part of the pulse ($2 \text{ s} < t < 3 \text{ s}$).

Gyrotron B5 (Fig. 5) starts also at a non-resonant frequency (about 770 MHz), undergoes transitions through the resonances at 720 MHz and 595 MHz, and finally stabilizes at a frequency of 555 MHz. As a result, most of the power is coupled to output 5 as well. The ratio of the powers detected by OUT1 and OUT5 during the last period of the pulse ($1 \text{ s} < t < 3 \text{ s}$) of 0.97 : 0.03 is in agreement with the expectations from the theoretical curves in Fig. 2. Additional experiments were performed by exchanging the role of B1 and B5, i.e. by tuning the resonance to 550 MHz, such that B1 was non-resonant and B5 was resonant, respectively. As expected, the power of both gyrotrons was coupled to output 1, however with somewhat less contrast for B5 due to its lower frequency stability.

For the power combination, both gyrotrons were switched on for pulse lengths of up to 10 s. The conditions were identical to the basic experiments described above. The result is shown in Fig. 6. Again, the gyrotrons B1 and B5 undergo one and two transitions through the resonances at 720 MHz and 595 MHz, respectively, until relative frequency stability is reached. After about 1 s, most of the power from both gyrotrons is coupled to output 5, with an average ratio of 0.945 : 0.055. Frequency jumps of the gyrotrons are imaged to the output signal. At the end of the pulse, the power in output 1 increases again, which is due to the frequency drift of gyrotron B1. The (integrating) power signals from the two calorimetric

loads (CCR1 and CCR5) at the outputs clearly confirm the power combination of the two beams into output 5. The comparison of the total input power into both channels measured from the calorimeters at the entrance of both transmission lines (930 kW) and the sum of the powers found in the CW loads (864 kW) yields a total transmission efficiency of 0.929. As the typical transmission efficiency for the mirror line to the CW loads is 0.97, the resulting efficiency for the diplexer averaged over both outputs is 0.958, which is in good agreement with low-power measurements [6] and eq. 1, if the additional ohmic loss of the matching mirrors is taken into account.

IV. SWITCHING EXPERIMENTS

Once the power of the two gyrotrons is combined to one output, the combined beam can be switched from one output to the other. This can be done in a relatively slow fashion by (i) moving one resonator mirror normal to its surface by about 0.48 mm resulting in a detuning of the resonator by 40 MHz. Then B1 becomes non-resonant and B5 becomes resonant (*cf.* Fig. 2), or (ii) by exchanging the gyrotron frequencies by increasing the power of B1 by about 110 kW and decreasing the power of B5 by the same amount. Both possibilities were confirmed by experiments.

Fast switching however is probably possible only by electronic frequency-shift keying of the gyrotrons by modulating one of the supply voltages. In a recent paper [6], switching of a single gyrotron (B1) beam was demonstrated, utilizing modulation of the body voltage in the range of $1 \text{ kV} \leq \Delta U_B \leq 5 \text{ kV}$ square wave with frequencies of $1 \text{ kHz} \leq f_{\text{MOD}} \leq 20 \text{ kHz}$. For the operational condition in these experiments, a frequency-shift keying of 25 MHz could be

obtained for $\Delta U_B = 4$ kV, $f_{MOD} = 5$ kHz, resulting in a high switching contrast of 94 % in the resonant and 99% in the non-resonant output.

First experiments on fast switching of the combined beam were performed, but for the parameters used here, a frequency modulation of only 10 MHz could be obtained applying modulation voltages of 4 kV (B5) and 5 kV (B1), respectively. Nevertheless, a proof-of-principle was possible: The gyrotrons were started without modulation. After 2.5 s, modulation for both gyrotrons was turned on. Note that the average power drops and thus the average frequency increases with the onset of power modulation. The power of the gyrotrons was adjusted such, that in the modulated period, B1 had an average frequency slightly above, and B5 a frequency slightly below the resonance at 595 MHz. This is shown in Fig. 7, where the frequencies of the gyrotrons are plotted as function of time. Fig. 7a shows the complete 5-s pulse for gyrotron B1, whereas Fig. 7b shows sections of a corresponding pulse with gyrotron B5 with modulation of 1 kHz and 5 kHz, respectively. With these conditions and a frequency shift keying in the same phase, the combined power is switched between both outputs. An example is given in Fig. 8, showing a 1 ms time window of a 5-s pulse in the stationary phase near to the pulse end. Note here that the power modulation due to the body voltage modulation was rather high, as can be seen from the power monitors IN1 and IN5. Therefore, the switching contrast, i.e. the ratio between minimum and maximum power in each output, is superimposed by the power modulation, giving a too high value for OUT 5 and a too low value for OUT1. This result is therefore considered as a proof-of principle for switching of a combined beam, but will not be analysed quantitatively. It is worth noting, that the limit for the switching frequency is given only by the slew rate of the body-voltage modulator, which for the present experiments is 600 V/ μ s, and switching could be demonstrated even at 20 kHz.

A stronger frequency change during modulation, preferably > 30 MHz, and a better control of the frequency of both gyrotrons would be advantageous for quantitative experiments. A careful optimization of the operating parameters of both gyrotrons to maximize the frequency change at minimum power modulation is considered a necessary prerequisite and is envisaged for the next step experiments.

In principle, the diplexer can be used to set any splitting ratio for the output power. To demonstrate this, we have modulated the two gyrotrons with different frequencies of 2 kHz (B1) and 1.05 kHz (B5), respectively, as seen from Fig. 9 (top). Depending on the relative phase of the modulation periods, 4 levels of the power are generated in output 5, which is depicted in Fig. 9 (bottom). The complementary behaviour is seen from output 1, the signal to noise ratio for this signal was, however, somewhat worse than for output 5.

V. Conclusion and future perspective

The present experiments with the quasi-optical high-power diplexer show good agreement with theory and demonstrate the possibility of power combination of two sources into one of two outputs, as well as fast switching of the combined power between the outputs.

The results show, that for highly efficient power combination, frequency stability of the gyrotrons is a critical issue. This means that for a real application – as long as no frequency-controllable gyrotrons are available – a control of the path length of the diplexer is advantageous, either pre-programmed on the basis of experience with the frequency drift of the corresponding gyrotrons or, preferably, automatic, e.g. by a "dither-stabilizer". Developments for real-time control of the diplexer resonance frequency have started [10].

Fast spontaneous frequency jumps will remain a problem within the response time of the control; however, a more broadband design of the diplexer would reduce this problem strongly. Note that for power combination with a resonant diplexer, the frequency of the resonance should follow the frequency of only one gyrotron; the frequency of the other source can vary as long as it is sufficiently separated from the resonances (see Fig. 2).

For switching applications with one gyrotron only at the input, problems of frequency drift can also be solved with a control of the resonant length. Within certain limits imposed by resonator loss and dimensions of the diplexer, the slope of the resonance can be designed such that a high switching contrast can be reached for a relatively small frequency-shift keying, which does not require too much voltage modulation with the concomitant loss.

The design of the "universal diplexer" which is appropriate simultaneously for power combination and switching of a combined power needs to be a careful compromise between a broadband solution which is tolerant to some frequency deviations and a narrow-band concept with good switching contrast even for small frequency-shift keying. For the operation with conventional gyrotrons, tools like variation of the frequency by adjusting the cooling water of the cavity (typ. 3 MHz/deg) or even by variation (usually meaning reduction!) of the power as was done in the proof-of principle experiments have to be applied.

Once frequency-controllable gyrotrons [11, 12, 13] are available, the wide range of applications of high-power diplexer would become available, including staggering of these devices for multiplexers [12].

In conclusion, the results motivate the development of power combiners and fast switches until maturity, taking into account the variety of possible solutions [5, 14, 15, 16, 17] for best performance, and the application at a fusion device; experiments at the tokamaks ASDEX Upgrade in Garching and FTU in Frascati are planned.

Acknowledgement

This work is carried out in the frame of the virtual institute "Advanced ECRH for ITER", (a collaboration between FZK Karlsruhe, IPP Garching and Greifswald, IPF Stuttgart, IAP Nizhny Novgorod and IFP Milano), which is supported by the Helmholtz-Gemeinschaft deutscher Forschungszentren. The ECRH system for W7-X used for this work is managed by the project PMW, ECRH for W7-X hosted at FZK Karlsruhe (collaboration between FZK Karlsruhe, IPP Garching and Greifswald, and IPF Stuttgart). The authors would like to thank the staff of the mechanical workshop at IPF Stuttgart for careful manufacturing of the diplexer equipment. Fruitful discussions with Alex Bruschi, including his proposal of combined switching are gratefully acknowledged.

Power combination of two 140 GHz gyrotrons and fast switching of the combined beam
by V. Erckmann et al

References

- [1] Design Description Document for the ITER ECRH System G 52 DDD 5 01-05-29 W 0.1
- [2] Zohm H, Gantenbein G, Giruzzi G, Günter S, Leuterer F, Maraschek M, Meskat J P, Peeters A G, Suttrop W, Wagner D, Zabiego M, and ASDEX-Upgrade Team, ECRH Group, Experiments on neoclassical tearing mode stabilization by ECCD in ASDEX Upgrade. *Nucl. Fusion* 39 (1999), 577 – 580
- [3] La Haye R J, Prater R, Buttery R J, Hayashi N, Isayama A, Maraschek M E, Urso L, and Zohm H, Cross-machine benchmarking for ITER of neoclassical tearing mode stabilization by electron cyclotron current drive. *Nucl. Fusion* 46 (2006) 451–461
- [4] Petelin M I and Kasperek W, Electrically controlled scanning of wave beam produced by gyrotron: Option for plasma fusion experiment. Proc. 6th Int. Vacuum Electronics Conference (IVEC 2005), Noordwijk, The Netherlands, p. 131
- [5] Kasperek W, Petelin M I, Erckmann V, Shchegol'kov D Yu, Bruschi A, Cirant S, Thumm M, Plaum B, Grünert M, Malthaner M, Fast switching and power combination of high-power electron cyclotron wave beams: principles, numerical results and experiments. *Fusion Sci. Technol.* 52 (2007), 281 – 290, and references therein
- [6] W Kasperek, M.I. Petelin, D.Yu Shchegolkov, V. Erckmann, B. Plaum, A. Bruschi, et al, A fast switch, combiner and narrow-band filter for high-power millimetre wave beams. *Nucl. Fusion* 48 (2008) 054010.
- [7] Erckmann V, et al., 2007, Electron Cyclotron Heating for W7-X: Physics and Technology. *Fusion Sci. Technol.*, 52 (2007) 291.
- [8] Thumm M et al., EU Megawatt-class 140-GHz CW gyrotron. *IEEE Trans. Plasma Sci.* 35 (2007) 143 - 153
- [9] Brand P and Müller G A, Circuit design and simulation of a HV-supply controlling the power of 140 GHz 1 MW gyrotrons for ECRH on W7-X. *Fusion Eng. Design* 66-68 (2003), 573 – 577
- [10] W. Bongers et al, *Fusion Sci Technol.*, submitted.
- [11] Golubiatnikov G Yu et al., Gyrotron frequency control by a phase lock system. *Technical Physics Letters* 32 (2006), 650-652
- [12] Petelin M I, Quasi-optics in High-Power Millimeter-Wave Systems. 6th Workshop on High Energy Density and High Power RF, WV, USA, AIP Conference Proc. 691 (2003), 251-262

- [13] Ilyakov E, et al., Gyroklystron operating at a sequence of high-order modes, in Strong microwaves in Plasmas, N. Novgorod, ed. by A.Litvak, 2006, Vol. 1, 58-61.
- [14] Smits F M A, 1993, Power combiners for incoherent waves. Proc. of 8th Joint workshop on ECE and ECRH, Report IPP III/186, Vol. 2, 607 – 621, 1993
- [15] Koshurinov Yu I, Pavelyev V G, Petelin M I, Turchin I V, Shchegol'kov D Yu, Diplexer based on open cavity with corrugated mirrors. Tech. Phys. Lett. 31 (2005) 709 - 711
- [16] Bruschi A, Cirant S, Moro A, Simonetto A, Beam Combination and Routing at High Power with a Ring-type Waveguide Millimeter-Wave Resonator, Fusion Sci. Technol. 53 (2008), 97 – 103
- [17] W. Wubie, W. Kasperek, and B. Plaum, Numerical and experimental investigations of a diplexer for combination and switching of high-power millimeter waves, Int. Conf. on Infrared and Millimeter Waves, Pasadena, 2008

Power combination of two 140 GHz gyrotrons and fast switching of the combined beam
by V. Erckmann et al

FIGURE CAPTIONS

Fig. 1:

Sketch for a high-power design of a resonant diplexer using a 4-mirror quasi-optical cavity with grating couplers.

Fig. 2:

Transmission functions of the diplexer as function of the absolute frequency (top scale) and as function of the frequency after the down-converter used in the gyrotron frequency measurements (bottom scale, *cf.* chapter 3). Blue dashed line: non-resonant, red solid line: resonant output.

Fig. 3:

Photograph of the diplexer installed in the beam duct of the ECRH system on W7-X. The input beams are coupled from the rear (mirrors MD1 and MD5) into the vertical resonator, the output beams are focussed to absorbing loads in the foreground (CCR1 and CCR5). Grating couplers on the last matching mirrors provide power signals for each output (OUT1 and OUT5).

Fig. 4:

Top: Temporal variation of the frequency of gyrotron B1 (start frequency is about 780 MHz + f_{LO}). Bottom: Temporal variation of the body voltage U_{B1} , the gyrotron power monitor IN1, and the two outputs OUT1 and OUT5 of the diplexer, when gyrotron B1 is pulsed at a power of 370 kW with pulse length of 3 s. Dashed lines used for channel 1, solid lines for channel 5.

Fig. 5:

Top: Temporal variation of the frequency of gyrotron B5 (start frequency is about 770 MHz + f_{LO}). Bottom: Temporal variation of the body voltage U_{B5} , the gyrotron power monitor IN5, and the two outputs OUT1 and OUT5 of the diplexer, when gyrotron B5 is pulsed at a power of 560 kW with pulse length of 3 s. Dashed lines used for channel 1, solid lines for channel 5.

Fig. 6:

Top: Temporal variation of the frequency of gyrotron B1 (start frequency is about 780 MHz + f_{LO}). Bottom: Temporal variation of the body voltage U_{B51} and U_{B5} , the gyrotron power monitors IN1 and IN5, and the two outputs OUT1 and OUT5 of the diplexer, when gyrotrons B1 and B5 are pulsed at a power of 370 kW and 560 kW with pulse length of 10.0 s and 9.6 s, respectively. Additionally, the power signals from the CW loads (CCR1 and CCR5) are shown. Note that the scale for the load power applies only for the steady state case. Dashed lines used for channel 1, solid lines for channel 5.

Fig.7:

Left: Frequency of the gyrotron B1 as function of time for the combined switching experiment.. Modulation is switched on at $t = 2.5$ s. Right: Same for gyrotron B5. Two time slices taken at $t > 3.0$ s show the relative position with respect to the diplexer resonance frequency with 1 kHz and 5 kHz modulation, respectively.

Fig. 8

Switching of the combined beam at 5 kHz switching frequency. Upper section: Body voltages U_{B1} and U_{B5} (thick lines), and power monitors IN1 and IN5 (thin lines). Lower section: Output power monitors OUT1 and OUT5. Dashed lines: channel 1, solid lines: channel 5.

Fig. 9:

Modulation of gyrotron B1 with $f_{\text{mod}} = 2$ kHz, $\Delta U_{B1} = 5$ kV, and gyrotron B5 with $f_{\text{mod}} = 1.05$ kHz, $\Delta U_{B1} = 4$ kV. Upper section: Body voltages U_{B1} and U_{B5} (thick lines), and power monitors IN1 and IN5 (thin lines). Lower section: Output power monitors OUT1 and OUT5. Dashed lines: channel 1, solid lines: channel 5.

Power combination of two 140 GHz gyrotrons and fast switching of the combined beam
by V. Erckmann et al

Fig. 1, Power combination ...V. Erckmann et al

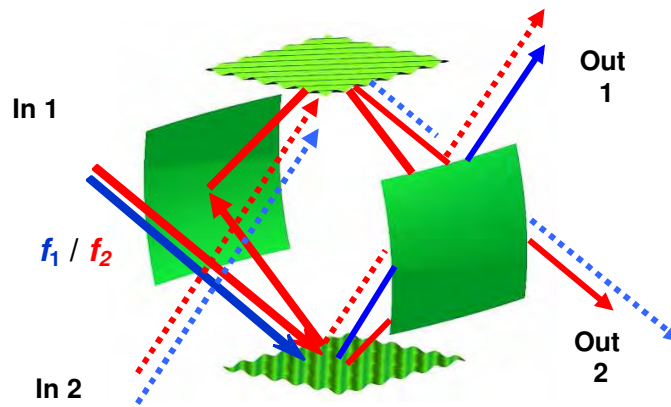


Fig. 2, Power combination ...

V. Erckmann et al

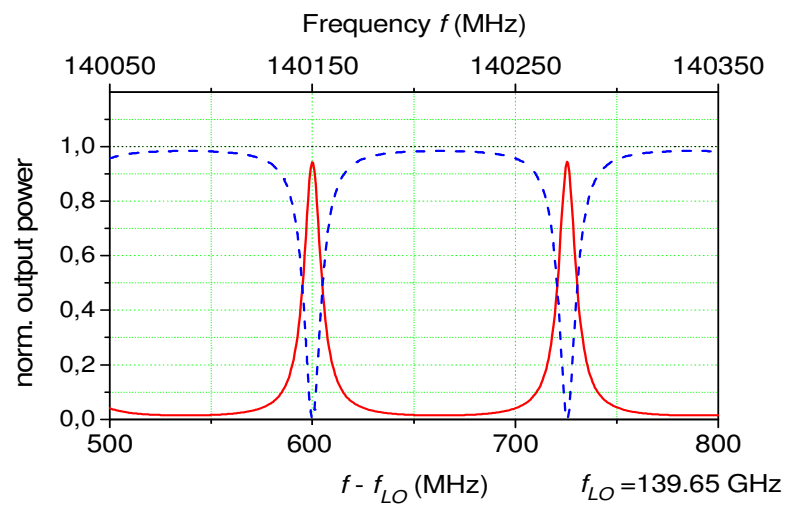


Fig. 3, Power combination ...

V. Erckmann et al

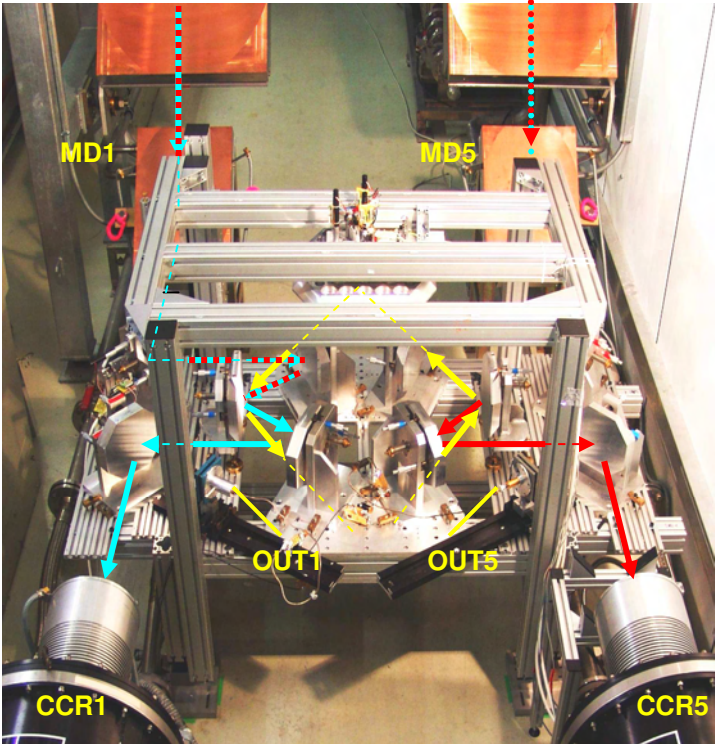
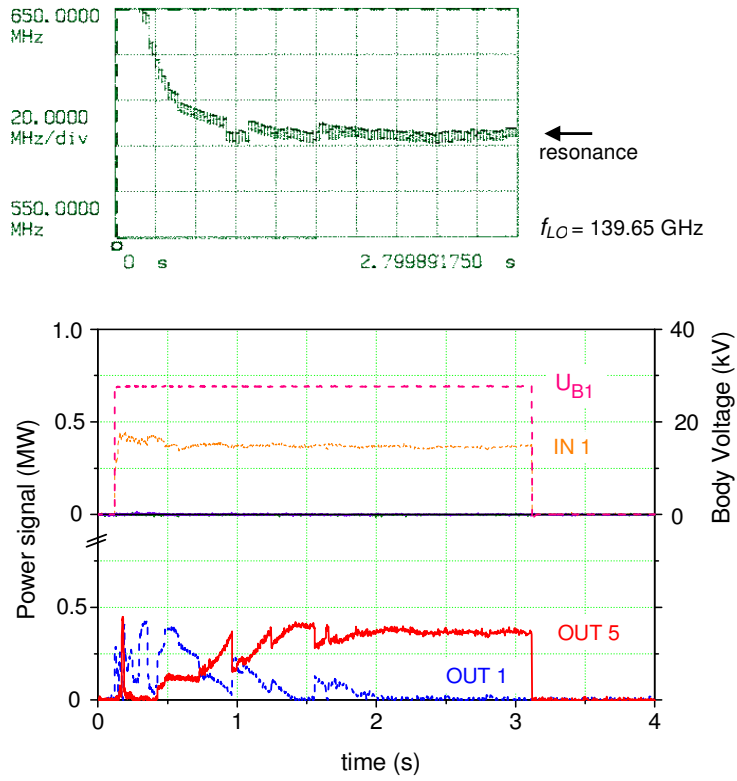


Fig. 4, Power combination ...

V. Erckmann et al



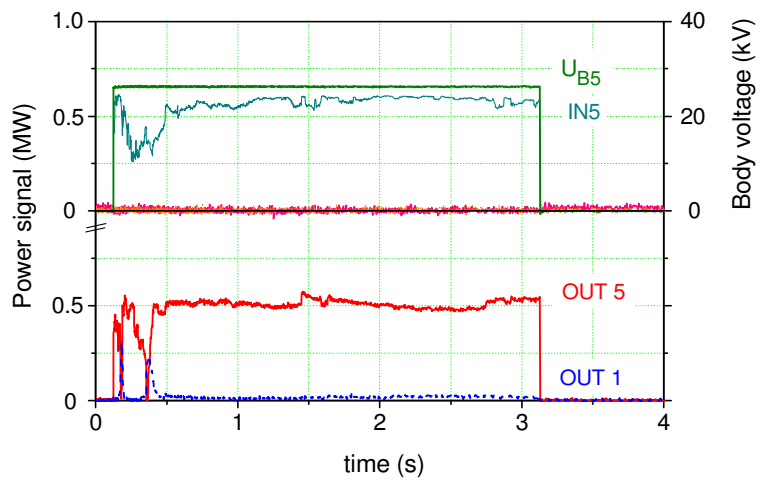
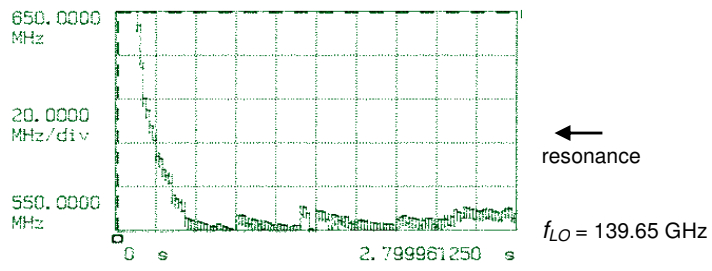


Fig. 6, Power combination ...

V. Erckmann et al

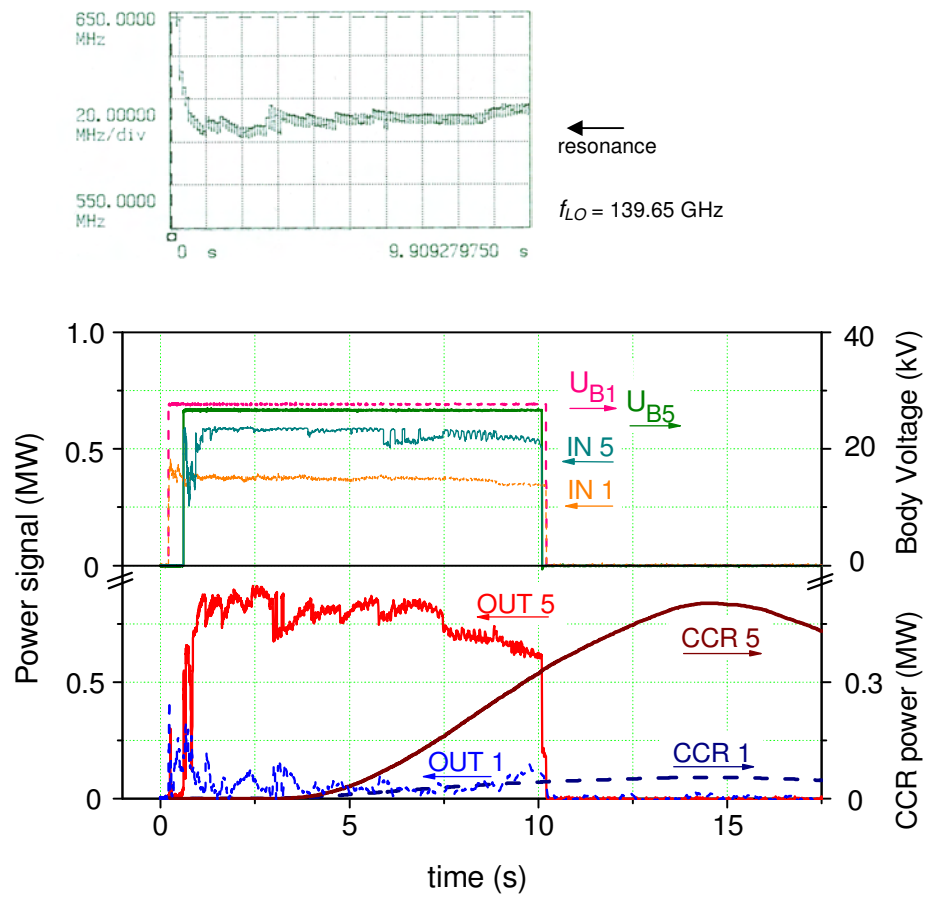


Fig. 7, Power combination ...

V. Erckmann et al

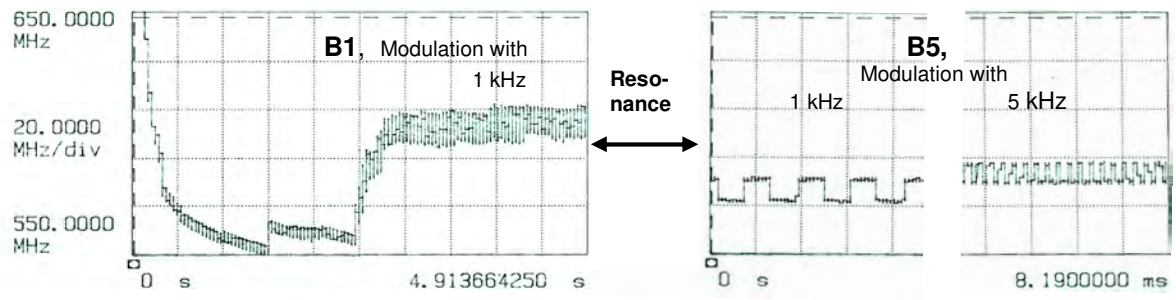


Fig. 8, Power combination ...

V. Erckmann et al

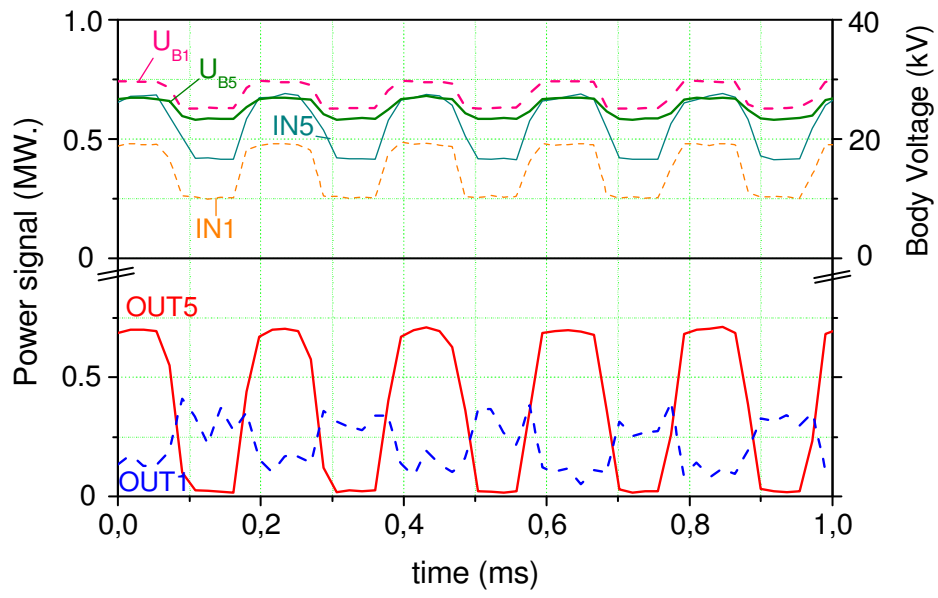


Fig. 9, Power combination ...

V. Erckmann et al

